
Article:
Norazman, F. orcid.org/0000-0002-5873-2955, Smith, P., Ellis, A. et al. (1 more author) (2017) Smoother and stronger high speed sintered elastomers through surface modification process. International Journal of Rapid Manufacturing, 6 (2/3). pp. 155-169. ISSN 1757-8817

https://doi.org/10.1504/IJRAPIDM.2017.10003091

Article:
Norazman, F., Smith, P., Ellis, A. et al. (1 more author) (2017) Smoother and stronger high speed sintered elastomers through surface modification process. International Journal of Rapid Manufacturing, 6 (2/3). p. 155. ISSN 1757-8817

https://doi.org/10.1504/IJRAPIDM.2017.10003091

Smoother and stronger high speed sintered elastomers through surface modification process

Farhana Norazman*[1], Patrick Smith[1], Adam Ellis[2], Neil Hopkinson[2]
fnorazman1@sheffield.ac.uk, patrick.smith@sheffield.ac.uk, adam.ellis@xaar.com, neil.hopkinson@xaar.com

[1]The University of Sheffield, Centre for Advanced Additive Manufacturing, North Campus Graduate Research Centre, Sheffield, S3 7HQ UK
[2]Xaar plc, 316 Science Park, Milton Road, Cambridge, CB4 0XR UK

*Corresponding author

Farhana Norazman is a PhD student at the University of Sheffield's Centre for Advanced Additive Manufacturing (AdAM). Her research focuses on polymer sintering using the High Speed Sintering process with interest in performance monitoring and evaluation.

Patrick J. Smith is a senior lecturer at the University of Sheffield. After obtaining his Ph.D. from Cambridge University in 2001, he worked as a post-doctoral researcher at the University of Manchester, England, the Technical University of Eindhoven, the Netherlands and the University of Freiburg, Germany. For the last twelve years, his research has been primarily concerned with applied inkjet printing. His group at Sheffield undertakes funded research into reactive inkjet printing, controlled crystallisation and polymer printing. Other research interests are involved with drying behaviour, inkjet used in tissue engineering, printed electronics and additive manufacture.

Adam Ellis received his Masters (2007) and PhD in Chemistry (2011) from the University of Sheffield. He was then an EPSRC doctoral prize fellow before moving to the Department of Mechanical Engineering to join the Centre for Advanced Additive Manufacturing at the University of Sheffield in 2012. Adam worked as a post-doctoral research associate until 2016 when he joined Xaar as project manager for 3D Services.

Neil Hopkinson is Director of 3D Printing at Xaar, UK and a visiting Professor at The University of Sheffield and has worked in 3D Printing / Additive Manufacturing since commencing his PhD in 1996.

ABSTRACT

High Speed Sintering is a novel additive manufacturing process which creates parts by employing a combination of inkjet printing and infrared heating to sinter successive layers of polymer powder. This paper investigates the effect of a new surface modification method called the PUSh™ process on the mechanical properties of high speed sintered elastomer. ALM TPE210-S elastomeric powder was used to manufacture specimens, and the PUSh™ process was subsequently performed on select specimens. Surface roughness and mechanical properties of TPE210-S specimens were measured. The results show that the PUSh™ process reduced surface roughness by 50% from 20 µm to 10 µm. Finished specimens had 50% higher values of ultimate tensile strength, Young's modulus and elongation at break compared to unfinished specimens, and tear strength was significantly improved by 233%. The process resulted in 3% average part shrinkage while part hardness remains unchanged. In overall, the mechanical properties of high speed sintered TPE210-S elastomer were improved by the PUSh™ process.

KEYWORDS

additive manufacturing; high speed sintering; HSS; powder bed fusion; polymer sintering; thermoplastic elastomers; surface modification; PUSh process; mechanical properties; surface roughness; shore hardness; tensile strength; Young's modulus; elongation at break; tear strength.

INTRODUCTION AND PROBLEM DEFINITION

Additive Manufacturing (AM) is a group of technologies which creates objects from 3D model data by joining raw material layer upon layer. Gibson et al. (2010) discussed the different methods used to classify AM processes, either by the physical state of raw material input or more commonly, the technology employed to fuse the material.

High Speed Sintering (HSS) process, according to the Wohlers Report (2015) is a combination process of powder bed fusion and binder jetting; two of the methods classified in ASTM F2792. The report also suggested the potential of HSS to compete with plastic injection moulding. However, surface roughness of parts manufactured by AM is still inferior compared to injection moulding parts. Previous research on the surface roughness of laser sintered nylon-12 parts reported values between 9 – 20 µm compared to 1 µm achieved by injection moulding (Bacchewar et al., 2007; Kruth et al., 2003).

This paper presents a new surface modification method, the PUSh™ process which improved the surface roughness of elastomer ALM TPE210-S parts. Parts made from this material generally have rougher surfaces compared to nylon-12. The manufacturing of elastomeric parts on the HSS machine is detailed and the effect of PUSh™ process on the mechanical properties of manufactured parts are discussed.

High Speed Sintering (HSS) Process

The HSS process is a relatively new AM technology which employs inkjet printing and infrared heating technologies to sinter polymer powder in creating three dimensional objects. Figure 1 shows a schematic diagram of the high speed sintering machine. The key components; an inkjet print head, an infrared lamp and a roller are all housed in the conveyor-operated

carriage which traverses the build platform. The build platform also holds a waste chute, alongside the feed bed and build bed, both of which move vertically throughout the build process.

HSS build process involves a series of pre-processing, building and post-processing steps. It starts with a 3D CAD model which is converted into an STL file, then further sliced into a stack of 2D images and converted into bitmaps. An optional greyscale value can be applied to the bitmaps before the files are transferred to the HSS machine. Build parameters are set on the machine and prepared powder is fed into the feed chamber to warm up. Once the machine is ready, a build can be started and build time is directly proportional to the number of z-layers (build height). A build starts with the carriage situated on the right hand side of the platform and the feed bed raised by a layer thickness. As the carriage moves left, the roller spreads fresh powder from the feed bed onto the build bed. The infrared lamp radiates over the build bed to prewarm the powder in this preheat stroke. When the carriage returns, the build bed is lowered and monochromatic bitmap images are printed in Radiation Absorbent Material (RAM) onto it. The infrared lamp provides instantaneous radiation and the RAM will absorb sufficient thermal energy to sinter the underlying powder. Surrounding powder will remain unsintered and act as a support to the build. This cycle is repeated until the build finishes. The part is then left to cool with all heating parts switched off, before the powder cake can be removed from the machine. Unsintered powder is removed from the part through bead blasting process and other post-processing techniques such as infiltration or surface enhancement may follow.

Early studies have been carried out to evaluate the processing of HSS. Hopkinson and Erasenthiran (2004) investigated the effect of adding carbon black to standard nylon powder on sintering time. They discovered that sintering time was lowered with increasing amount of carbon black, due to the thermal conduction by carbon black particles to their surrounding powder. Thomas et al. (2006) reported that the thermal energy from the build bed heater and infrared lamp influenced the unsintered powder bed hardness differently. A balance between the two different heat sources was necessary to enable easy powder removal from manufactured parts. Majewski et al. (2007) proceeded to quantify the effect of bed temperature and infrared lamp power on tensile properties and unsintered powder bed hardness. The results showed that an increase in both parameters corresponded to higher tensile strength, Young's Modulus, elongation at break and unsintered powder bed hardness. Majewski et al. (2008) found that in high speed sintering, higher lamp power had a greater effect on part shrinkage in z direction.

More recent studies have been performed to assess the influence of ink used on the mechanical properties of manufactured specimens. Fox et al. (2015) suggested that the use of an alternative ink from a different supplier produced parts with a comparable performance to the parts printed using standard HSS ink. Extensive research on varying the volume of ink deposited via the introduction of greyscale has also been conducted. Figure 2 shows an example of greyscale level with corresponding colour. The greyscale level ranges from 0 to 255 and different levels were applied when manufacturing parts from Nylon-12 and TPE210-S powder (Ellis et al., 2014; 2015a). Results showed that the tensile properties of parts generally improved with decreasing level of greyscale (higher volume of ink) up until powder degradation occurred, where the properties started to worsen. The optimum greyscale level which yielded the best tensile properties for TPE210-S was found to be at greyscale 57.

Additive Manufactured Elastomers

Harper (2002) states that elastomers are widely used in the automotive sector to produce parts such as exhaust mounts and air ducts. Many attempts have been undertaken to process elastomers by AM, such as the oxygen mask seal made on a modified Fused Deposition Modelling printer by Elkins et al. (1997) and Objet TangoBlackPlus dogbones printed on an Objet Connex 350 (Moore and Williams, 2008).

TPE210-S, supplied by Advanced Laser Materials (2011) is designed to be used with Laser Sintering (LS), and its properties can be found in Table 1. Earlier studies by Vasquez et al. (2011) and Davidson (2012) have been successful in manufacturing TPE210-S on laser sintering machines. Laumer et al. (2015) has also used the TPE in simultaneous laser beam melting process, alongside polyethylene to produce a multi-material part.

The tensile properties achieved by high speed sintering TPE210-S parts have been shown to be superior to equivalent laser sintered parts and exceed the values specified by the manufacturer. Norazman and Hopkinson (2014) investigated the addition of fumed silica to the powder mix, which further improved the tensile strength, Young's modulus and elongation at break of manufactured TPE210-S parts. Ellis et al. (2015a) explored the application of greyscale to produce elastomeric parts with comparable tensile properties. Table 2 details the tensile values obtained from these studies, where the elongation at break values more than doubled the laser sintered equivalent.

PUSh™ Process

The PUSh™ process was developed to address the poor quality of surfaces on additive manufactured parts. The process is a chemical surface treatment and surface analysis shows no chemical residue is left in the part. Its application is material specific instead of process specific, and it has had success with nylon derivatives and other elastomers. Previous research showed that the process has a positive influence on the mechanical properties of high speed sintered Nylon-11 (Ellis et al., 2015b).

Figure 3 shows the transformation of a specimen when PUSh™ process was applied to it. It can clearly be seen that the process significantly improves aesthetic appeal. The finish on the part transforms from matte to glossy. The change in colour of the specimen can be attributed to the black ink contained in the specimen, which is made prominent after the surface treatment.

EXPERIMENTAL PROCEDURES

This section will provide an overview of the experimental procedures used in this study. These include an initial powder characterisation, manufacture of specimens on the High Speed Sintering (HSS) machine, application of PUSh™ post-processing technique and finally mechanical testing performed on the specimens.

Powder Characterisation

A thermal analysis was performed on the feed powder using Differential Scanning Calorimetry (DSC) method. The DSC test was carried out on a double furnace PerkinElmer DSC8500 instrument and according to ASTM D3418 standard. 0.0113g of powder sample was tested against an empty pan. The sample was heated from 20°C to 210°C at 20°C per minute, then held at 210°C for one minute. The sample was then cooled down to 20°C at the same rate and held for another one minute. This cycle was run twice before a thermal profile could be plotted. The thermal profile obtained was used to determine HSS process window and to set the build parameter values.

Manufacture of HSS Specimens

In this study, twenty five test specimens consisting of three different geometries; A, B and C were manufactured on the bespoke HSS machine. Figure 4 shows the CAD models of all specimen type and their dimensions. Specimen A was an ASTM type I compression set test piece, specimen B was an ASTM D638 type V tensile test piece and specimen C was a type C tear strength test piece conforming to ASTM D624. The number of test specimens manufactured for each specimen A, B and C was five, ten and ten respectively.

The HSS machine was equipped with standard HSS ink and standard HSS 2kW infrared lamp. The feed material, TPE210-S powder used was 100 percent virgin. The build images were set to a greyscale level of 57 with a layer thickness of 0.1mm. All builds were orientated on the xy plane and used the same set of build parameters listed in Table 3. These build parameters had been optimised for processing TPE210-S based on both its thermal profile and general HSS experimental observations.

Testing of HSS Specimens

The dimensions of each manufactured specimen were measured using a Vernier calliper. Three measurements were taken for each dimension and the mean calculated. The measurements were performed before and after the PUSh™ process, and any change in dimension in x, y and z directions was calculated.

Surface roughness test was performed on each test specimen A on a Mitutoyo Surftest contact profilometer rig at 1.0 mm/s speed over 15.0 mm profile length. Average surface roughness, R_a of bottom and top surfaces of each specimen were measured five times and the mean calculated.

Each test specimen A was tested for Shore A hardness using Sauter HBA 100-0 handheld durometer according to ASTM D2240 standard. Five measurements were taken for each specimen and a mean value was calculated.

Tensile testing in accordance with ASTM D638 was performed on test specimens B under 1,000 N load at a rate of 10 mm/min. The values of ultimate tensile strength, Young's modulus and elongation at break were obtained and compared against all specimens.

Test specimens C were subjected to tear tests operated under 100 N load at 12 mm/min in accordance with ASTM D624 standard. Tear strength values were recorded from the tests.

PUSh^{TM} Process Application on HSS Specimens

The PUSh^{TM} surface finish was applied to all five specimens A (disc) after the initial dimension measurement, surface roughness and hardness test. Five of each test specimen B (tensile) and C (tear) were set aside, measured and finished before being tested accordingly. The exact details of the process application cannot be disclosed due to intellectual property restrictions.

RESULTS AND DISCUSSION

This section reports the findings from the experiments performed. The material's thermal properties and the manufactured HSS specimens' dimensions, surface roughness, and mechanical properties are presented and discussed.

Thermal Properties

Figure 5 shows the thermal profile obtained from the DSC test of virgin TPE210-S elastomer. The crystallisation temperature is observed at 50°C. The melt temperature, T_m is observed between 130°C to 140°C, which is lower than the manufacturer provided value of 178°C. The glass transition temperature, T_g can be observed between 100°C to 120°C.

There was a lack of sharp peak for both melt and glass transition temperatures. This suggested that TPE210-S underwent gradual changes over the range of temperatures. The temperature range between T_g and T_m was commonly called "the process window", and the determination of this range was vital in order to set the HSS build parameters. Based on this thermal profile, TPE210-S had a narrow process window and gradual softening/hardening region, which indicated that processing this material would be more difficult compared to material with clear temperature peaks e.g. Nylon-12.

Dimensional Analysis

Figure 6 illustrates the average change in dimensions for all test specimens in x, y, and z directions. The dimensional changes for each specimen are measured to observe the effect of PUSh^{TM} process on dimensional accuracy. An overall decrease in dimension (shrinkage) can be observed for all specimens across all directions after the application of PUSh^{TM} process.

Specimen A experiences a consistent average part shrinkage by about 2% across all axes. Specimen B shrinks at 2.3%, 3.7% and 4.2% across x, y, and z axes respectively. On the other hand, part shrinkage in specimen C is more random at 1.6%, 1.8% and 7.8% across x, y, and z axes respectively. This difference in degree of shrinkage could be attributed to the shape of the test specimens. Specimen A and B were compact in shape while specimen C had a more slender geometry. This suggested that compact shapes are more favourable to receive a uniform treatment across all directions due to the manual application of the PUSh^{TM} process.

Surface roughness

In HSS, surfaces parallel to the xy plane are commonly called bottom and top surfaces. Bottom surfaces are downward-facing (closer to the build bed base) and top surfaces are upward-facing (closer to the build bed surface).

Figure 7 shows the average surface roughness, R_a values for bottom and top surfaces of test specimens A before and after the surface modification, i.e. unfinished and PUSh respectively. The unfinished specimens have an average R_a of 20 μm and 36 μm on the bottom and top surfaces, respectively. After PUSh, the average R_a for the surfaces are now 10 μm and 18 μm. Due to the unavailability of data on the surface roughness of additive manufactured elastomer, a direct comparison could not be made for this material.

It can be observed from Figure 7 that the PUSh™ process results in a significant reduction in R_a values on both surfaces. The average R_a for finished specimens is halved that of unfinished. Low R_a values imply smoother surfaces and are more desirable in manufacturing consumer products. The consistent improvement of surface roughness on both surfaces and the small error suggest that the PUSh™ process is effective in smoothing surfaces in all directions.

In common with most AM powder bed processes, the R_a values of HSS specimens vary between part surfaces resting on different planes. In HSS case, the bottom surface is generally smoother than the top surface. This difference may be attributed to the distribution of new layer of powder above the top surface, where loose unsintered powder may adhere thus producing a rough surface. It could also be due to the meniscus formed on the bottom surface which led to a smoother surface.

Hardness

Figure 8 presents the shore A hardness values of the disc test specimens A. On a hardness scale of 0 to 100, the average shore hardness for unfinished and PUSh specimens is 54 and 53 respectively. There was very little difference between the two values, hence it can be inferred that the PUSh™ process had no effect on specimen's hardness.

Tensile Properties

Figure 9 exhibits the stress-strain curves obtained from the ASTM D638 tensile testing of one unfinished and one PUSh specimen. The values of Ultimate Tensile Strength (UTS), Young's modulus and elongation at break were extracted from these curves. The difference in shape of both curves suggests that the two set of specimens had failed differently. Figure 10, Figure 11 and Figure 12 show the UTS, Young's modulus and elongation at break values for all specimens, respectively.

The result shows that the average UTS for finished specimens is higher compared to unfinished specimens at 1.2 MPa and 0.8 MPa. The finished specimens are also stiffer, with a modulus of 6.2 MPa compared to the unfinished with 4.0 MPa. Similar trend can be observed with elongation at break values where the finished specimens break at 167% compared to a lower value of 103% in unfinished specimens.

The thermal profile of TPE210-S suggested that the material had an amorphous chain configuration. This was further reflected in the brittle failure of the unfinished specimens as

seen in Figure 9. On the other hand, PUSh specimens seemed to be sufficiently ductile to exhibit necking and experience a delayed fracture, as suggested by Daniels (1989). As a result, the PUSh specimens were generally 50% stronger compared to unfinished specimens.

Tear strength

Figure 13 compares the stress-strain curves gathered from the ASTM D624 tear testing, where both curves appear to be similar in shape. It can clearly be seen that PUSh specimens have a higher break stress at 1.4 MPa compared to 0.5 MPa of unfinished specimens.

Figure 14 shows the average tear strength values of test specimens B. The average tear strength of unfinished specimens is 6 kN/m while it is 20 kN/m for PUSh specimens. It is interesting to note that the surface finish has led to an improvement in tear strength by 233%.

Based on the surface analysis, it can be theorised that the mechanisms of the PUSh^{TM} process only acted on the surface of a specimen without changing its bulk density. A possible explanation for the improvement in tear strength was that the process had helped to seal any flaw on the specimen, thus a higher load was required to initiate tear on the finished specimens.

CONCLUSIONS

Surface finish of additive manufactured polymer parts, especially in powder bed fusion processes was generally poor compared to injection moulded parts, thus need to be enhanced. The PUSh^{TM} process, a new post-processing technique to improve surface quality of additive manufactured polymer parts was introduced. High speed sintered elastomer specimens were post-processed and their mechanical properties tested.

Results showed that the PUSh^{TM} process had successfully reduced surface roughness values by 50% on all surfaces. The process resulted in part shrinkage by an average of 3% and had no significant effect on part hardness. All mechanical properties were improved as a result of the PUSh^{TM} process. Ultimate tensile strength, Young's modulus and elongation at break values were higher by 50% while tear strength was dramatically improved by 233%.

The PUSh^{TM} process was previously proven to work on Nylon-12, Nylon-11, TPU and TPE210-S parts manufactured by any AM processes. The process was efficient in smoothing parts uniformly across all directions, however shrinkage should be taken into consideration when designing parts to be post-processed.

ACKNOWLEDGEMENTS

The authors gratefully acknowledge the financial support provided by Philips Research with special thanks to Dave Beaumont and Joyce van Zanten for supporting this work.

REFERENCES

Advanced Laser Materials. TPE210-S [Online]. http://alm-llc.com/Tech_Data_Sheets/TPE_210_S.pdf (Accessed 2 November 2015).

Bacchewar, P. B., Singhal, S. K. & Pandey, P. M. (2007) 'Statistical modelling and optimization of surface roughness in the selective laser sintering process', Proceedings of the Institution of Mechanical Engineers, Part B: Journal of Engineering Manufacture, Vol. 221**,** pp. 35-52.

Daniels, C. A. (1989) 'Tensile Properties', in Polymers: Structures and Properties, Technomic Pub. Co., Lancaster, PA, USA, pp. 43 - 50.

Davidson, C. (2012) Investigating the suitability of laser sintered elastomers for running footwear applications. PhD Thesis, Loughborough University, Loughborough, United Kingdom.

Elkins, K., Nordby, H., Janak, C., Gray, R., Bøhn, J. & Baird, D. (1997), 'Soft elastomers for fused deposition modeling' in Proc. 8th Solid Freeform Fabrication Symposium, pp. 441-448.

Ellis, A., Noble, C. J. & Hopkinson, N. (2014) 'High Speed Sintering: Assessing the influence of print density on microstructure and mechanical properties of nylon parts', Additive Manufacturing, Vol. 1**,** pp. 48-51.

Ellis, A., Hartley, L. & Hopkinson, N. (2015a) 'Effect of Print Density on the Properties of High Speed Sintered Elastomers', Metallurgical and Materials Transactions A, Vol. 46**,** pp. 3883-3886.

Ellis, A., Brown, R. & Hopkinson, N. (2015b) 'The effect of build orientation and surface modification on mechanical properties of high speed sintered parts', Surface Topography: Metrology and Properties, Vol. 3**,** pp. 034005.

Fox, L., Ellis, A. & Hopkinson, N. (2015), 'Use of an Alternative Ink in the High Speed Sintering Process' in 2015 Solid Freeform Fabrication Symposium, Proceedings of the 26th Solid Freeform Fabrication Symposium, The University of Texas at Austin, Austin, Texas, pp. 456-463.

Gibson, I., Rosen, D. W. & Stucker, B. (2010) Additive Manufacturing Technologies: Rapid Prototyping to Direct Digital Manufacturing, 2, Springer, New York.

Harper, C. A. (2002) 'Elastomeric Materials and Processes', in Handbook of Plastics, Elastomers, and Composites, Fourth Edition, McGraw Hill Professional, Access Engineering, pp.

Hopkinson, N. & Erasenthiran, P. (2004), 'High Speed Sintering – Early Research into a New Rapid Manufacturing Process' in Proceedings of the 15th Solid Freeform Fabrication Symposium, The University of Texas at Austin, Austin, Texas, pp. 312 - 320.

Kruth, J. P., Wang, X., Laoui, T. & Froyen, L. (2003) 'Lasers and materials in selective laser sintering', Assembly Automation, Vol. 23**,** pp. 357-371.

Laumer, T., Stichel, T., Gachot, A., Amend, P. & Schmidt, M. (2015) 'Realization of multi-material polymer parts by simultaneous laser beam melting', Journal of Laser Micro/Nanoengineering, Vol. 10**,** pp. 140-147.

Majewski, C. E., Hobbs, B. S. & Hopkinson, N. (2007) 'Effect of bed temperature and infra-red lamp power on the mechanical properties of parts produced using high-speed sintering', Virtual and Physical Prototyping, Vol. 2**,** pp. 103-110.

Majewski, C. E., Oduye, D., Thomas, H. R. & Hopkinson, N. (2008) 'Effect of infra-red power level on the sintering behaviour in the high speed sintering process', Rapid Prototyping Journal, Vol. 14**,** pp. 155-160.

Moore, J. P. & Williams, C. B. (2008), 'Fatigue characterization of 3D printed elastomer material' in 19th Annual International Solid Freeform Fabrication Symposium, Austin, TX, pp. 641-655.

Norazman, F. & Hopkinson, N. (2014) 'Effect of Sintering Parameters and Flow Agent on the Mechanical Properties of High Speed Sintered Elastomer', Journal of Manufacturing Science and Engineering, Vol. 136**,** pp. 061006.

Thomas, H. R., Hopkinson, N. & Erasenthiran, P. (2006), 'High Speed Sintering - Continuing research into a new Rapid Manufacturing process' in Proceedings of the 17th Solid Freeform Fabrication Symposium, The University of Texas at Austin, Austin, Texas, pp. 682-691.

Vasquez, M., Hopkinson, N. & Haworth, B. (2011), 'Laser Sintering Processes: Practical Verification of Particle Coalescence for Polyamides and Thermoplastic Elastomers ' in ANTEC 2011 Plastics: Annual Technical Conference Proceedings, Society of Plastics Engineers, Boston, pp. D41.

Wohlers Associates (2015) 'The future of additive manufacturing', in Wohlers Report 2015: 3D Printing and Additive Manufacturing State of the Industry Annual Worldwide Progress Report, Wohlers Associates Inc, Colorado, pp. 263-264.

Figures

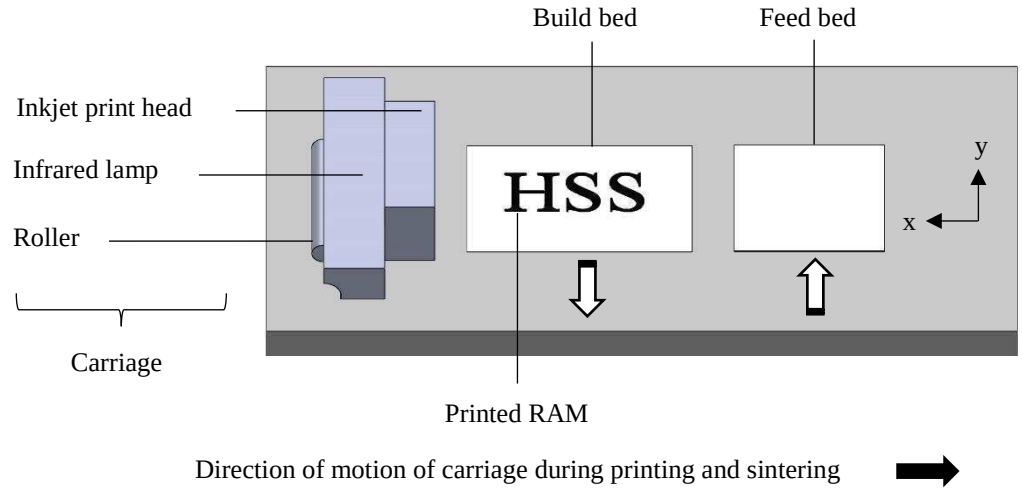

Figure 1: High speed sintering process

Figure 2: Greyscale value showing black (0) to white (255)

Figure 3: The PUSh™ process effect on specimen: before (left) and after (right)

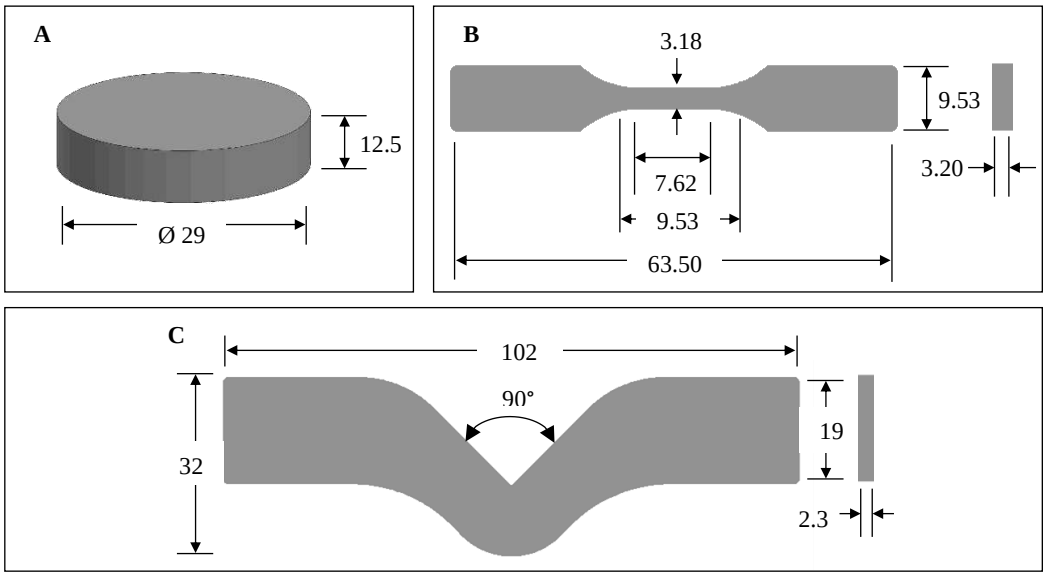

Figure 4: HSS specimens and dimensions in mm

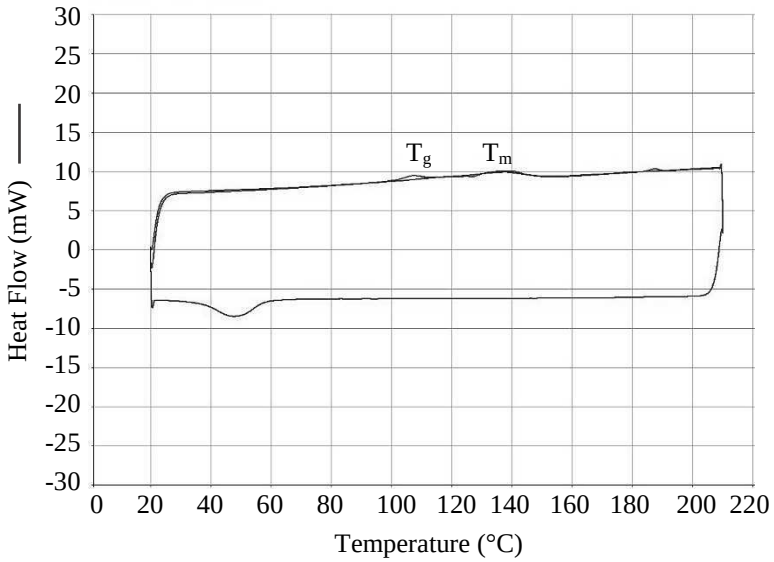

Figure 5: Thermal profile of TPE210-S elastomer

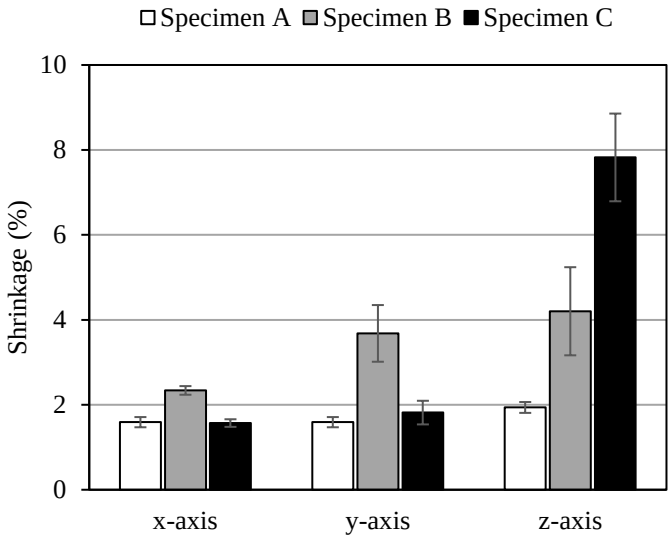

Figure 6: Effect of surface modification on HSS elastomer dimensions

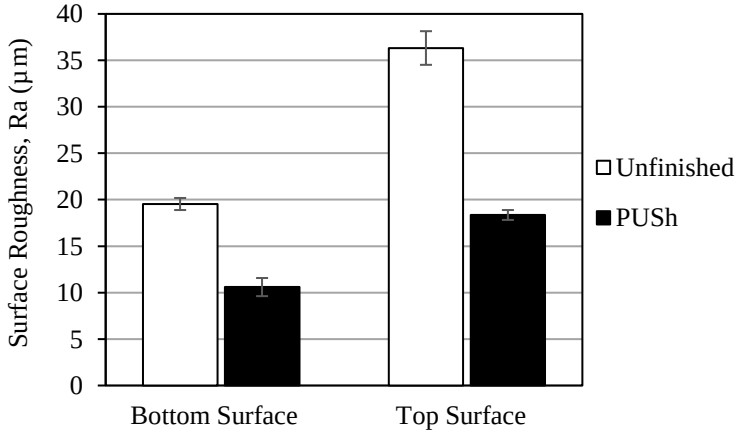

Figure 7: Effect of surface modification on the surface roughness of HSS elastomer surfaces

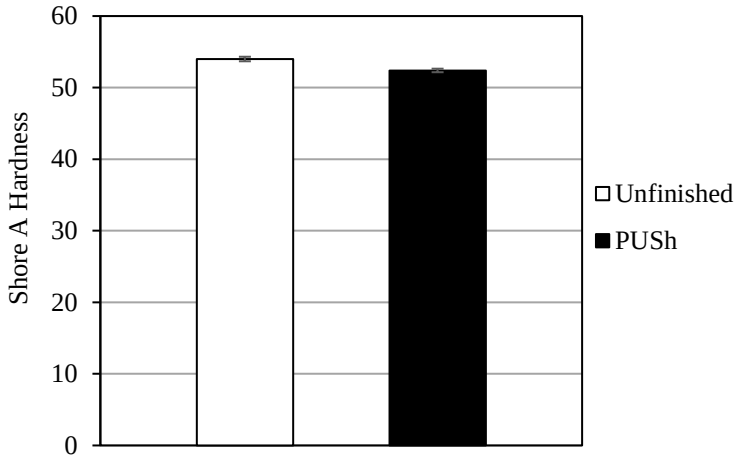

Figure 8: Effect of surface modification on HSS elastomer hardness

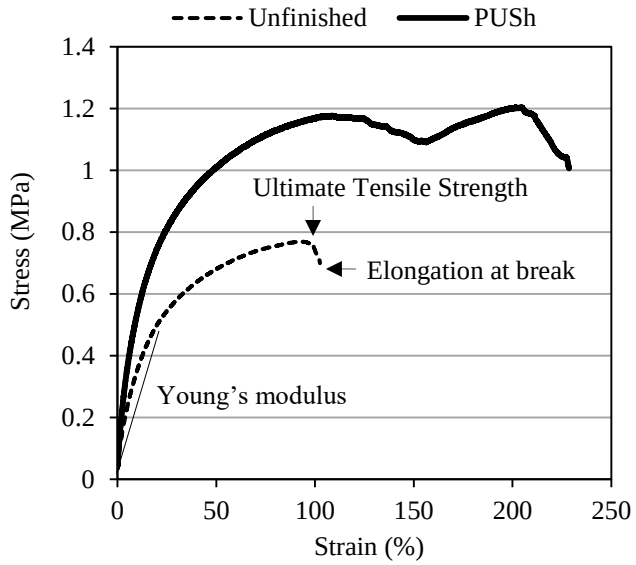

Figure 9: Tensile test curves for unfinished and PUSh specimens

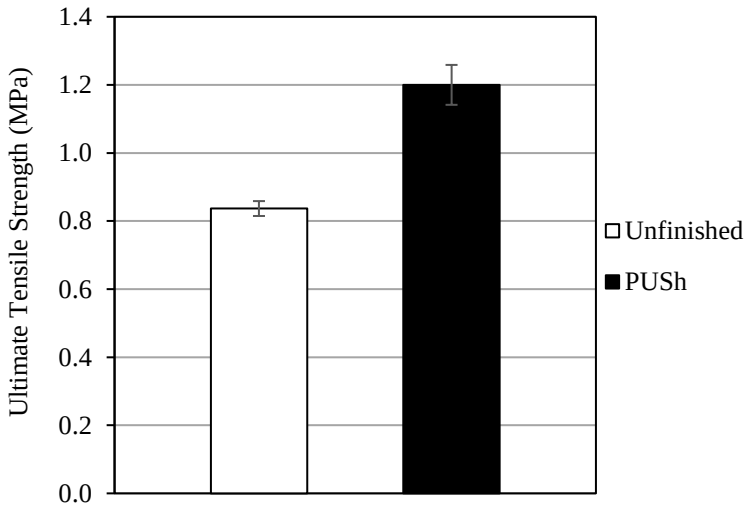

Figure 10: Effect of surface modification on HSS elastomer ultimate tensile strength

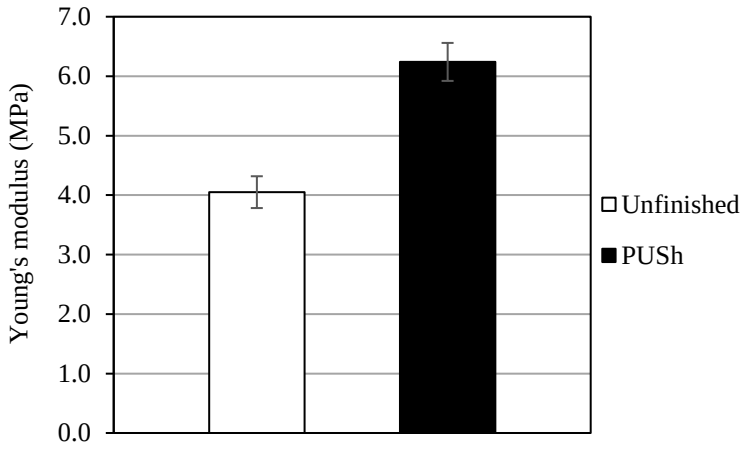

Figure 11: Effect of surface modification on HSS elastomer Young's modulus

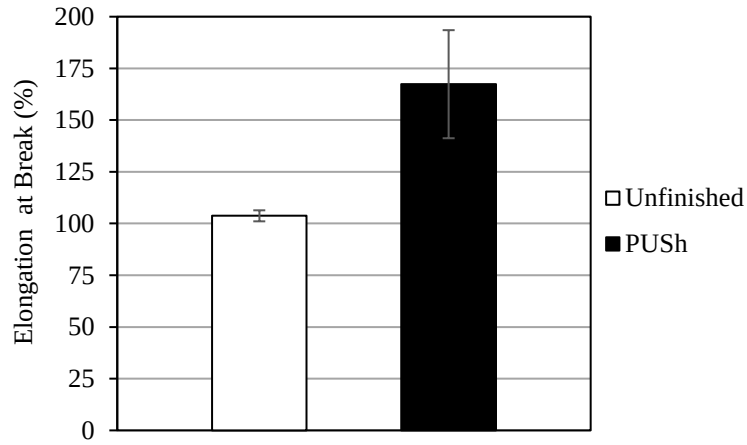

Figure 12: Effect of surface modification on HSS elastomer elongation at break

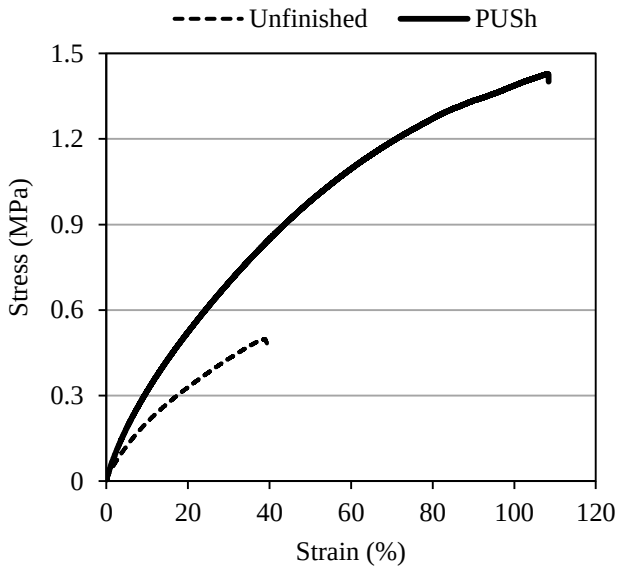

Figure 13: Tear test curves for unfinished and PUSh specimens

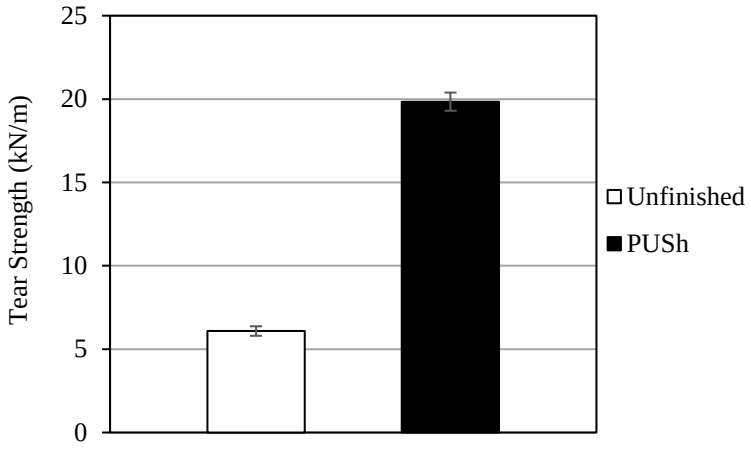

Figure 14: Effect of surface modification on HSS elastomer tear strength

Tables

Table 1: Laser-sintered TPE210-S elastomer material properties

Properties	Test Method	Value
Average particle size (D50)	Laser Diffraction	85 µm
Melting point	ASTM D3418	178°C
Shore hardness	ASTM D2240	40A
Ultimate Tensile Strength	ASTM D638	N/A
Young's modulus	ASTM D638	8 MPa
Elongation at Break	ASTM D638	110%

Table 2: High speed sintered TPE210-S elastomer properties

Material	Ultimate Tensile Strength (MPa)	Young's modulus (MPa)	Elongation at Break (%)
TPE mix 0.2% w/w Cab-O-Sil	2.57	10.90	284
TPE at Greyscale 57	3.10	12.50	248

Table 3: High speed sintering build parameter values

Parameter	Value
Build bed jacket (°C)	60
Build bed overhead (°C)	110
Feed bed jacket (°C)	28
Feed bed overhead (°C)	32
Preheat stroke (% at mm s^{-1})	40 at 80
Sintering stroke (% at mm s^{-1})	60 at 80